PII: S0032-3861(96)00858-0

Polymer Vol. 38 No. 12, pp. 3085–3089, 1997

0032-3861/97/$17.00 + 0.00

Preparation of high modulus nylon 46 fibres by high-temperature zone-drawing

Akihiro Suzuki* and Akira Endo
Department of Applied Chemistry and Biotechnology, Faculty of Engineering, Yamanashi University, 4-3-11 Takeda, Kofu, 400 Japan
(Received 19 April 1996; revised 25 July 1996)

The high-temperature zone-drawing (HT-ZD) method was applied to nylon 46 fibres to improve their mechanical properties. The HT-ZD treatments were carried out three times at different temperatures between 200 and 235°C. The draw ratio and crystallinity increased stepwise with the processing, and those of the HT-ZD3 fibre were 5.6 times and 51%, respectively. The HT-ZD3 fibre finally obtained had a Young's modulus of 7.2 GPa and a tensile strength of 1.0 GPa. The dynamic storage modulus (E') increased stepwise with the processing as well and was 8 GPa at 25°C for HT-ZD3 fibre. © 1997 Elsevier Science Ltd.

(Keywords: high-temperature zone-drawing; nylon 46 fibre)

INTRODUCTION

To produce high-modulus and high-strength nylon fibres, many techniques have been proposed. Dry-spinning[1], spinning from nylon 6/lithium chloride or nylon 6/lithium bromide mixtures[2,3], solid-state coextrusion of nylon-6 gel[4], and zone-drawing/-annealing[5] are some techniques leading to high-modulus and high-strength fibres. The high-temperature zone-drawing (HT-ZD) method was also proposed as a way to improve the mechanical properties of fibres. The HT-ZD treatment is carried out near to the melting point under the optimum applied tension to transform the lamellae present in as-spun fibres into extended chain crystals. The morphological changes in the crystallites can be expected to increase the number of tie molecules as intercrystalline bridges and then to improve the crystal continuity in the chain-axis direction. The increment in the degree of the crystal continuity is attributed to the high-modulus[6]. The HT-ZD method has been already applied to various crystalline polymers[7–10] and succeeded in producing fibres and films with high-modulus and high-strength.

Nylon 46 offers attractive properties in its high melting temperature and high crystallinity, compared with nylon 6 and nylon 66. The properties originate from a highly symmetrical molecular structure and fairly high amide groups content per unit length of chain compared with other nylons[11,12]. However, the high melting temperature of 295°C and high crystallinity make it difficult to draw as-spun nylon 46 fibres up to higher draw ratios. Because of the reduced drawability of nylon 46 the mechanical properties of nylon 46 are inferior to those of nylon 6 and nylon 66. So far nylon 46 has been little used in industry, and there were comparatively few studies of nylon 46 during the last decade[13–18], especially aimed at improving mechanical properties, compared with other nylons.

In this study, the HT-ZD method was applied to nylon 46 fibres to improve the mechanical properties. The HT-ZD treatments were carried out three times at different temperatures between 200 and 235°C. We measured the density, crystallite size, crystallites orientation factor, crystallinity, melting point, tensile and viscoelastic properties for the fibre obtained at each treatment. The changes in the superstructure and mechanical properties with the treatments were studied.

*To whom correspondence should be addressed

EXPERIMENTAL

Material

The original material used in the present study was as-spun nylon 46 fibre supplied by Unitika Ltd. The as-received fibre had a diameter of 0.327 mm and a crystallinity of 32%. The fibre was opaque because it contained a small amount of TiO_2. The original fibre was found to be isotropic by a wide angle X-ray diffraction photograph.

High-temperature zone-drawing

High-temperature zone-drawing (HT-ZD) was introduced in our earlier publications[2–4]. The apparatus used for HT-ZD treatment was specially constructed to draw fibre or film by local heating and is shown schematically in *Figure 1*. This apparatus consists of a zone heater of about 2 mm thickness and a Linead motor capable of moving the zone heater at an arbitrary speed. The HT-ZD is carried out by moving the zone heater along the drawing direction under an optimum tension.

Measurement

The draw ratio was determined in the usual way by measuring the displacement of ink marks placed 10 mm apart on the specimens before drawing. The density was measured at 23°C by the flotation method using a mixture of toluene and carbon tetrachloride.

The d.s.c. curves were recorded on a Rigaku d.s.c. connected to TAS 200 system at a heating rate of 10°C min^{-1} in a nitrogen gas atmosphere. The heat of fusion (ΔH_f) was obtained from the area of the melting

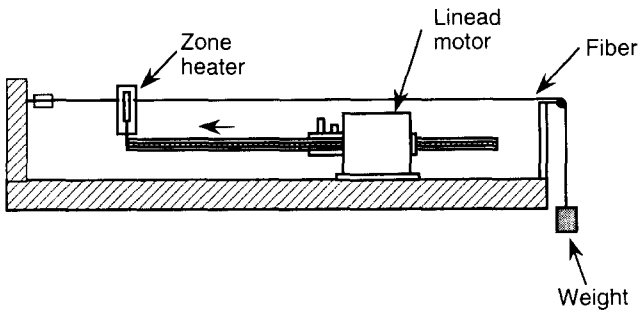

Figure 1 Scheme of the apparatus used for high-temperature zone-drawing

peak. To estimate the degree of crystallinity (X_c) from ΔH_f, it is assumed[19] that the heat of fusion (ΔH_0) for the completely crystalline nylon 46 has the same value as that for the nylon 6 (55 cal g^{-1}). The X_c was calculated by equation (1):

$$X_c = (\Delta H_f / \Delta H_0) \times 100 \quad (1)$$

The thermal shrinkage was measured with a Rigaku SS-TMA at a heating rate of 5°C min^{-1}. The specimens were 15 mm in length and were applied with a load of 5 g cm^{-2} which is the minimum value required to stretch the specimen tightly.

The orientation factor of crystallites was evaluated using the Wilchinsky[20] method with wide angle X-ray diffraction patterns. From the broadening of the diffraction peaks, the apparent crystal size was estimated by applying Scherrer's equation:

$$D_{hkl} = K\lambda / (\Delta\beta \cos\theta_{hkl}) \quad (2)$$

where D_{hkl} is the crystallite width normal to (hkl) plane, λ is the X-ray wavelength (1.542 Å), θ_{hkl} is the Bragg angle of the (hkl) plane, $\Delta\beta$ is the half-width of the peak and was made the correction for the instrumental broadening, and $K = 0.9$ in this experiment.

The tensile properties were determined on a Tensilon tensile testing machine (Orientec Co. Ltd). Young's modulus, tensile strength, and elongation at the break were determined from the stress–strain curves obtained at 25°C, RH 65%. The dynamic viscoelastic properties were measured at 110 Hz with a dynamic viscoelastometer Vibron DDV-II (Orientec Co. Ltd). The measurement was carried out over a range of temperature from 25 to about 250°C at a heating rate of 2°C min^{-1} in a stream of nitrogen gas.

RESULTS AND DISCUSSION

Conditions for the high-temperature zone-drawing

To determine the optimum conditions for the HT-ZD treatments, the fibres were drawn under various applied tensions at different drawing temperatures. The optimum conditions were decided from the relation between the drawing conditions and Young's moduli of the fibres obtained under various conditions; the condition where a high modulus was obtained was chosen as an optimum one for each treatment. *Table 1* lists the optimum conditions for the first HT-ZD (HT-ZD1), second HT-ZD (HT-ZD2), and third HT-ZD (HT-ZD3). Although we attempted a fourth HT-ZD (HT-ZD4) treatment, the Young's modulus could not be improved further by the HT-ZD4 treatment.

Table 1 Optimum conditions for high-temperature zone-drawing

	Drawing temperature (°C)	Applied tension (MPa)	Heater speed (mm min^{-1})
HT-ZD1	200	27.0	30
HT-ZD2	225	116.8	30
HT-ZD3	230	245.2	30

Table 2 Draw ratio (λ), density (d), crystallite orientation factor (f_c), and crystallite sizes (D_{hkl}) of (100) and (010) planes for the original and HT-ZD fibres

Fibre	λ	d (g cm^{-3})	f_c	D_{100} Å	D_{010} Å
Original	—	1.173	—	—	—
HT-ZD1	3.9	1.176	0.949	28.8	26.1
HT-ZD2	4.4	1.178	0.951	28.8	28.9
HT-ZD3	5.6	1.180	0.961	28.8	29.9

Superstructure for the HT-ZD fibres

Table 2 summarizes the draw ratio, density (d), crystallinity (X_c), crystallites orientation factor (f_c), and crystallite sizes normal to the (100) and the (010) planes (D_{100} and D_{010}) for the HT-ZD fibres. The outer (010) reflection is mixed with (110); for convenience, we refer to this as (010) only. The d and X_c increased stepwise with the processing and finally attained 1.180 g cm^{-3} and 51% for the HT-ZD3 fibre having a draw ratio of 5.6. The increment of d may be attributed to the orientation of the amorphous phase and the crystallization. However, the changes in d of the amorphous phase due to drawing are expected to be negligible, except when the amorphous phase is highly oriented in the drawing direction[21–23]. Therefore, the increment of d with the processing is mostly attributable to further crystallization during the treatments[24]. D_{010} increased from 26.1 to 29.9 Å, and D_{100} was held constant at 28.8 Å throughout the processing. Crystal growth in two directions, the a and b crystal axes, could hardly take place with the processing. Although the increase in d and X_c implies crystallization during treatments, the crystallite sizes normal to the (100) and (010) planes did not increase with the processing. This suggests that the increase in a number of crystallites and/or the crystal growth along the c axis take place during the treatments. Peszkin *et al.*[25] reported on the basis of WAXD and SAXS results that the growth of the crystals in the oriented fibre took place along the fibre axis of the crystal already oriented. The f_c of the HT-ZD1 fibre already reaches a high value close to unity, and the subsequent treatments show a slight improvement in the f_c.

Figure 2 shows a d.s.c. curve for each of the original and HT-ZD fibres. The original fibre shows two clearly distinguishable melting peaks: a high melting peak at 283°C and a low one at 270°C. Double melting peaks are attributed to the difference in the crystalline morphology; the high melting peak and the low one are based on a folded-chain crystal and an extended-chain crystal, respectively[26]. The melting peak of the HT-ZD1 fibre is located at 277°C and has a well defined shoulder on the high temperature side of its peak. In the d.s.c. curves for the HT-ZD2 and HT-ZD3 fibres, there are no shoulders, and the only single peaks are observed at 279 and 283°C, respectively. The melting peak shifts toward a higher

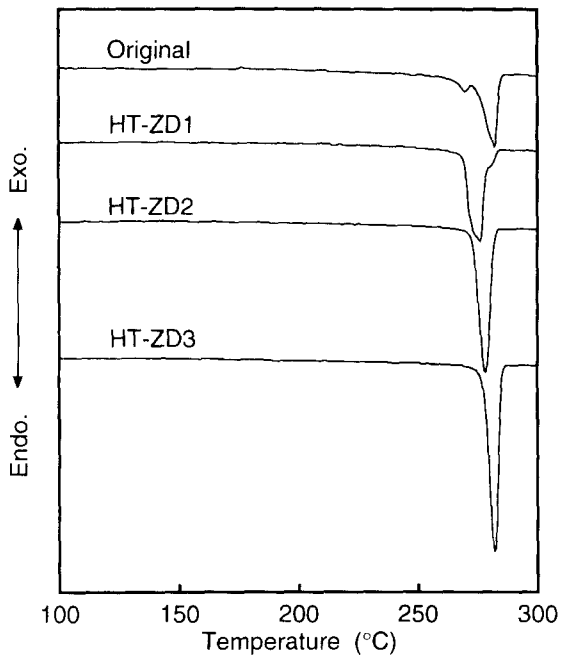

Figure 2 D.s.c. curves for the original and HT-ZD fibres

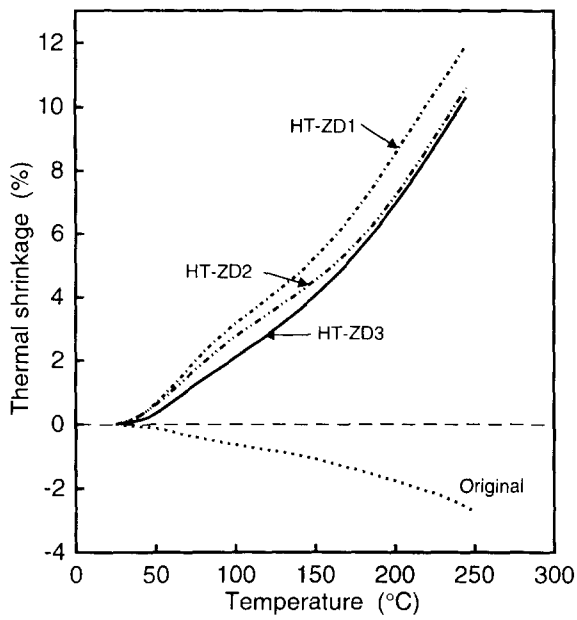

Figure 3 T.m.a. curves for the original fibre and HT-ZD fibres: (----), original; (— - —), HT-ZD1; (— - - —), HT-ZD2; (———), HT-ZD3

temperature and becomes sharper with the processing. The changes in the profile of the melting peaks were attributed to an increase in the degree of perfection of the crystallites[27,28].

Figure 3 shows the t.m.a. curves for various fibres. Although the original fibre extends with increasing temperature, the HT-ZD fibres shrink with temperature. The degree of thermal shrinkage at 250°C for the HT-ZD1 fibre was 12%, those for both the HT-ZD2 and HT-ZD3 fibres were about 10%. The thermal shrinkage during heating is associated with chain folding in the amorphous regions[29] and increases as the draw ratio increases[30]. In spite of an increase in the draw ratio, the shrinkage for the HT-ZD fibres decreases with the processing. This implies that the thermal shrinkage closely depends on the degree of crystallinity rather than the draw ratio. More specifically, the crystallites acting as physical crosslinks are thought to inhibit the large-scale segmental motion responsible for the transition[31].

Mechanical properties of the HT-ZD fibres

The tensile properties of the HT-ZD fibres obtained under the optimum conditions are summarized in *Table 3*. The Young's modulus and tensile strength increase stepwise with the processing. The HT-ZD3 fibre finally obtained has a Young's modulus of 7.2 GPa and a tensile strength of 1.0 GPa. The Young's modulus is higher than that of the commercial fibres[11] (3.9 GPa), whilst the tensile strength is nearly equal to that of the commercial fibres[11]. Nakamae *et al.*[32] reported that the elastic modulus E_1 of the crystalline regions of nylon 46 in the direction parallel to the chain axis was 48 GPa at room temperature. The Young's modulus of the HT-ZD3 fibre corresponds to 15% of the E_1, and there is a considerable gap between the achieved modulus and the E_1 value. However, the rate of attainment to the E_1 value is higher than that of other nylons because the E_1 of nylon 46 is smaller than those of nylon 6 ($E_1 = ca\ 160$ GPa)[33] and nylon 66 ($E_1 = 176$ GPa)[34].

Figure 4 shows the temperature dependence of the dynamic storage modulus (E') for the original and the HT-ZD fibres. The E' values increase progressively with processing over a wide temperature range as well as the increment of Young's modulus. In the HT-ZD3 fibre finally obtained, the maximum E' value at 25 reaches 8.2 GPa and is higher than the E' value (about 3.6 GPa at room temperature) reported by Kudo *et al.*[17]. The E'

Table 3 Tensile properties for the original and HT-ZD fibres

Fibre	Young's modulus (GPa)	Tensile strength (GPa)	Elongation at break (%)
Original	1.2	—	—
HT-ZD1	5.6	0.7	24.8
HTZD2	6.5	0.9	21.7
HT-ZD3	7.2	1.0	10.3

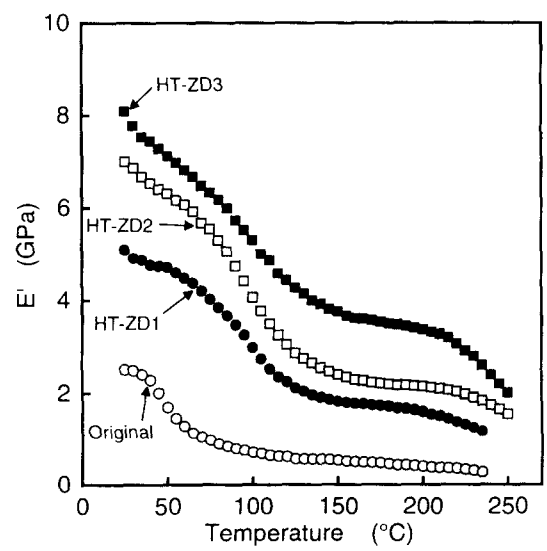

Figure 4 Temperature dependence of the storage modulus (E') for the original fibre and HT-ZD fibres: (○), original; (●), HT-ZD1; (□) HT-ZD2; (■), HT-ZD3

values of all the fibres decrease gradually up to the onset of an α relaxation with increasing temperature. The α relaxation originates with the rupture of interchain hydrogen bonding due to the motions of chain segments in the amorphous regions[35]. The modulus falls markedly in the α relaxation process with temperature. However, the E'–temperature curves clearly show a plateau in the temperature range 150–200°C, and the plateau moduli are about 3.6 GPa for the HT-ZD3 fibre.

Figure 5 shows the temperature dependence of tan δ for the original and HT-ZD fibres. The original fibre shows the α relaxation peak at 75°C. The loss maximum of the α relaxation peak shifts to a higher temperature, its peak decreases in height progressively, and becomes much broader with the processing. The HT-ZD3 fibre has a peak value of 0.05 at 115°C. The changes in position and in profile of the loss peak show that the thermal mobility of molecules in the amorphous regions is gradually restricted as they become surrounded by crystallites that grew with the processing. In the nylon 46 the α relaxation is found at 10–20°C higher temperatures than in other nylons because of the fairly high amide groups content compared with other nylons[11,12].

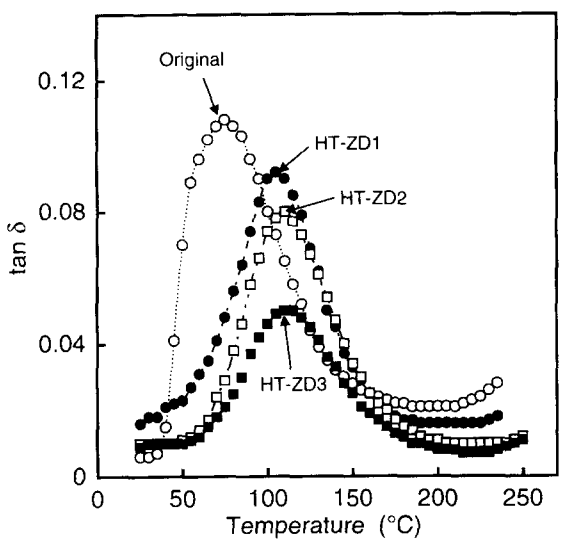

Figure 5 Temperature dependence of tan δ for the original fibre and HT-ZD fibres: (○), original; (●), HT-ZD1; (□), HT-ZD2; (■), HT-ZD3

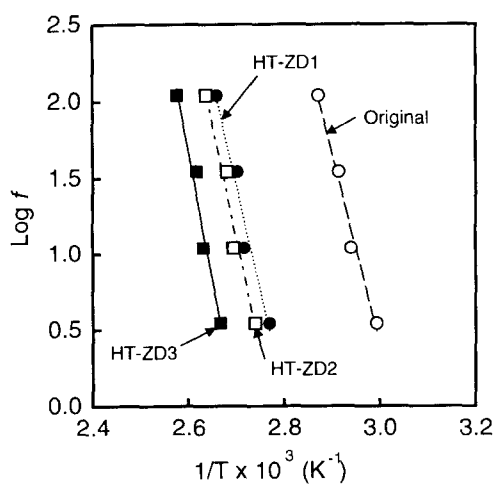

Figure 6 Plots of log f vs $1/T$ for the original fibre and HT-ZD fibres: (○), original; (●), HT-ZD1; (□), HT-ZD2; (■) HT-ZD3

Table 4 Activation energy (ΔH) of α dispersion for the original and HT-ZD fibres

Fibre	ΔH (kcal mol^{-1})
Original	57.9
HT-ZD1	63.7
HT-ZD2	69.0
HT-ZD3	78.1

Figure 6 shows the plots of log f vs the reciprocal temperature ($1/T$), where T is the peak temperature of the α relaxation at a frequency f in the tan δ spectra. Since all experimental data for each fibre are approximately on straight lines, the activation energies can be calculated from the slopes of lines by using the Arrhenius equation. The resulting activation energies are summarized in *Table 4*. The activation energy increases from 57.9 kcal mol^{-1} for the original fibre to 78.1 kcal mol^{-1} for the HT-ZD3 fibre. The increase in the activation energy suggests that the associations among the chains in the amorphous regions become stronger with processing.

CONCLUSION

We applied the high-temperature zone-drawing (HT-ZD) method to nylon 46 fibres to improving their mechanical properties. Our experimental data discussed here led to the conclusion that the HT-ZD method is effective in improving the mechanical properties of nylon 46 fibres in the same manner as other crystalline polymers.

REFERENCES

1. Gogolewski, S. and Pennings, A. J., *Polymer*, 1985, **26**, 1394.
2. Aciernmo, D., La Mantia, F. P., Polizotti, G., Alfonso, G. C. and Ciferri, A., *J. Polym. Sci., Polym. Lett. Edn*, 1977, **15**, 323.
3. Richardson, A. and Ward, I. M., *J. Polym. Sci., Polym. Phys. Edn*, 1981, **19**, 1549.
4. Chuah, H. H. and Porter, R. S., *Polymer*, 1986, **27**, 1022.
5. Kunugi, T., Suzuki, A. and Hashimoto, M., *J. Appl. Polym. Sci.*, 1981, **26**, 213.
6. Gibson, A. G., Davies, G. R. and Ward, I. M., *Polymer*, 1978, **19**, 683.
7. Kunugi, T., *J. Polym. Sci. Polymer Lett.*, 1982, **20**, 329.
8. Kunugi, T., Kawasumi, T. and Ito, T., *J. Appl. Polym. Sci.*, 1990, **40**, 2101.
9. Kunugi, T., Suzuki, A. and Kubota, E., *Kobunshi Ronbunsyu*, 1992, **49**, 161.
10. Suzuki, A., Maruyama, S. and Kunugi, T., *Kobunshi Ronbunsyu*, 1992, **49**, 741.
11. Mochizuki, M. and Kudo, K., *Sen-i Gakkaishi*, 1991, **47**, P336.
12. Steeman, P. A. M. and Maurer, F. H. J., *Polymer*, 1985, **26**, 1394.
13. Roerdink, E. and Warnier, J. M. M., *Polymer*, 1985, **26**, 1582.
14. Gaymans, R. J., Aalto, S. and Maurer, F. H. J., *J. Polym. Sci., Part A: Polym. Chem.*, 1989, **27**, 423.
15. Atkins, E. D. T., Hill, M., Hong, S. K., Keller, A. and Organ, S., *Macromolecules*, 1992, **25**, 917.
16. Butle, A. M. W., Folkers, B., Mulder, M. H. V. and Smolders, C. A., *J. Appl. Polym. Sci.*, 1993, **50**, 13.
17. Kudo, K., Mochizuki, M., Kiriyama, S. Watanabe, M. and Hirami, M., *J. Appl. Polym. Sci.*, 1994, **52**, 861.
18. Shah, Pravin L., *Polym. Eng. Sci.*, 1994, **34**, 759.
19. Roerdirnk, E. and Wanier, J. M. M., *Polymer*, 1985, **26**, 1852.
20. Wilchinsky, Z. W., *J. Appl. Phys.*, 1959, **30**, 792.
21. Salem, D. R., *Polymer*, 1992, **33**, 3182.
22. LeBourvellec, G., Monnerie, L. and Jarry, J. P., *Polymer*, 1986, **27**, 856.

23. Nobb, J. H., Bower, D. I. and Ward, I. M., *Polymer*, 1976, **17**, 25.
24. Gaymans, R. J., Van Utteren, T. E. C., Van der Berg, J. W. A. and Schultz, J. M., *J. Polym. Sci. Polym. Chem. Ed.*, 1977, **15**, 537.
25. Peszkin, P. N., Schultz, J. M. and Lin, J. S., *J. Polym. Sci. Polym. Phys. Ed.*, 1986, **24**, 2592.
26. Elenga, R., Seguela, R. and Rietsch, F., *Polymer*, 1974, **15**, 277.
27. Wills, A. J., Capaccio, G. and Ward, I. M., *J. Polym. Sci. Polym. Phys. Ed.*, 1980, **18**, 493.
28. Gaymans, R. J., Van Utteren, T. E. C., Van Der Berg, J. W. A. and Schuyer, J., *J. Polym. Sci. Polym. Chem. Ed.*, 1977, **15**, 537.
29. Wilson, M. P. W., *Polymer*, 1974, **15**, 277.
30. Choy, C. L., Leung, W. P. and Ong, E. L., *Polymer*, 1985, **26**, 884.
31. Ghanem, M. A. and Porter, R. S., *J. Polym. Sci. Part B*, 1989, **27**, 2587.
32. Nishino, T., Tada, K. and Nakamae, K., *Polym. Preprints, Jpn*, 1991, **40**, 1263.
33. Sakurada, I. and Kaji, K., *J. Polym. Sci. Part C*, 1970, **31**, 57.
34. Nakamae, K., Nishino, T., Hata, K. and Matsumoto, T., *Kobunshi Ronbunsyu*, 1987, **44**, 421.
35. Papir, Y. S., Kapur, S., Rogers, C. E. and Baer, E., *J. Polym. Sci.*, 1972, **10**, 1305.